THE JOURNAL OF PHYSICAL CHEMISTRY C

Article

pubs.acs.org/JPCC

Development of Hybrid Silver-Coated Gold Nanostars for Nonaggregated Surface-Enhanced Raman Scattering

Andrew M. Fales,[†,‡] Hsiangkuo Yuan,[†,‡] and Tuan Vo-Dinh*[,†,‡,§]

[†]Fitzpatrick Institute for Photonics, [‡]Department of Biomedical Engineering, and [§]Department of Chemistry, Duke University, Durham, North Carolina 27708, United States

Supporting Information

ABSTRACT: In the ongoing search for ever-brighter surface-enhanced Raman scattering (SERS) nanoprobes, gold nanostars (AuNSs) have emerged as one of the best geometries for producing SERS in a nonaggregated state. Despite their high enhancement factor, optical extinction from plasmon-matched nanoparticles can greatly attenuate the overall SERS intensity. Herein, we report the development of a new hybrid bimetallic NS-based platform that exhibits superior resonant SERS (SERRS) properties. In this new nanoplatform, coating AuNSs with a subtotal layer of silver (AuNS@Ag) can further increase their SERRS brightness by an order of magnitude when being interrogated by an off-resonant excitation source. Silica-encapsulated AuNS@Ag nanoprobes were injected intradermally into a rat pelt, where SERRS was readily detected with higher signal-to-noise than nanoprobes prepared from AuNS. Moreover, these off-resonance AuNS@Ag nanoprobes did not cause any gross photothermal damage to tissue, which was observed with the plasmon-matched AuNSs. This novel SERRS-active hybrid nanoprobe exhibits high SERRS brightness and offers promising properties for future applications in sensing and molecular imaging.

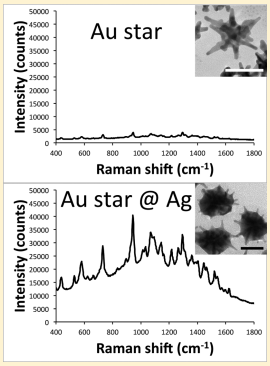

1. INTRODUCTION

In recent years, much effort has been devoted to the development of nanoparticles with the brightest SERS possible. While spherical gold and silver colloids have long been used in SERS studies, aggregation is typically required to generate the "hotspots" of electromagnetic field for high SERS enhancement. Although this can give extremely low limits of detection, reproducibility becomes an issue when aggregation is relied upon.[1,2] To overcome this problem, nanoparticles with intrinsic hotspots, such as nanorods and AuNSs, can be employed. AuNSs exhibit superior SERS properties owing to their tunable plasmon, for matching the excitation wavelength, and multiple sharp branches, each with a strongly enhanced electromagnetic (EM) field localized at its tip.[3−5]

Our laboratory has extensively characterized the electromagnetic properties of AuNSs and their use in SERS.[5−7] We have previously developed AuNS-based SERS nanoprobes for *in vitro* applications[8−10] and are now interested in developing *ex vivo*[11] and *in vivo* applications, which present several challenges. The first issue we observed was the extremely high attenuation of SERS signal when attempting to detect the particles through tissue. The second issue found was the efficient photothermal transduction of AuNS solution, causing unwanted localized thermal trauma. It was interesting to note that when using a commercially available SERS nanoprobe based on aggregated AuNPs, the signal attenuation due to self-absorption was lower and heating of the solution after laser excitation was minimal. Such phenomena can be explained by the mismatch between the extinction maximum of these nanoparticles and the wavelength of the incident laser, hence limiting photothermal transduction and self-absorption of the Raman scattered light. Other reports have recently shown that plasmon matching is not as desirable as once thought when performing SERS measurements in solution.[11,12] It was therefore of interest for us to develop highly SERS active (i.e., highest brightness factor) nanoparticles without the aforementioned disadvantages.

Two strategies were employed in this study. One is to use resonant dyes to generate resonant SERS (SERRS). The other is to modify the composition and plasmon band of the nanoparticles to enhance their optical properties. Silver coating is a well-known method to blue-shift the surface plasmon resonance and increase the SERS activity of gold nanoparticles. This process allows the monodisersity of gold nanoparticles to be preserved while taking advantage of the superior optical properties of silver. Although silver coating has previously been applied to various gold nanoparticles, there have been no reports about the coating of silver on AuNSs for making SERS nanoprobes.[13] Herein, we describe a method to coat AuNSs with different amounts of silver, resulting in an order of magnitude increase in SERS brightness. By blue-shifting the plasmon of the particles, there is a significant decrease in the amount of self-absorption and transduced heat when irradiating with a NIR laser. The optimal silver coating on AuNS was found to occur immediately before the branches were completely embedded into the silver shell. These silver-coated gold nanostars (AuNS@Ag) were used to make silica-coated SERS nanoprobes that were injected into rat skin *ex vivo* to demonstrate the potential of using this novel SERS platform in biological applications.

Received: September 12, 2013
Revised: January 7, 2014
Published: January 14, 2014

2. EXPERIMENTAL SECTION

2.1. Materials. Gold(III) chloride trihydrate ($HAuCl_4 \cdot 3H_2O$), L(+)-ascorbic acid (AA), tetraethyl orthosilicate (TEOS), trisodium citrate dihydrate, sodium borohydride ($NaBH_4$), 1 N hydrochloric acid solution (HCl), hexadecyltrimethylammonium bromide (CTAB, product H9151), Dulbecco's phosphate buffered saline (PBS), *O*-[2-(3-Mercaptopropionylamino)ethyl]-*O*′-methylpoly(ethylene glycol) (mPEG-SH, MW 5K), 4-mercaptobenzoic acid (pMBA), IR-780 iodide, 3,3′-diethylthiadicarbocyanine iodide (DTDC), 3,3′-diethylthiatricarbocyanine iodide (DTTC), and 1,1′,3,3,3′,3′-hexamethylindotricarbocyanine iodide (HITC) were purchased from Sigma-Aldrich (St. Louis, MO) at the highest purity grade available. Silver nitrate ($AgNO_3$, 99.995%) was supplied by Alfa Aesar (Ward Hill, MA). Ammonium hydroxide (NH_4OH, 29.5%), carbon-coated copper TEM grids, 1 mL disposable syringes, 27G × $^1/_2$ in. needles, and 200 proof ethanol (EtOH) were obtained through VWR (Radnor, PA). All glassware and stir bars were thoroughly cleaned with *aqua regia* and dried prior to use. Ultrapure water (18 MΩ·cm) was used in all preparations.

2.2. Instrumentation. Raman spectra were recorded with a PIXIS:100BReX CCD mounted to a LS-785 spectrograph (1200 grooves mm^{-1} grating), controlled by LightField software, from Princeton Instruments (Trenton, NJ). A 785 nm diode laser was fiber-coupled to an InPhotonics RamanProbe (Norwood, MA) for excitation, with a power of 150 mW at the sample; the collection fiber of the RamanProbe was coupled to the entrance slit of the LS-785 spectrograph. Absorption spectra were collected with a FLUOstar Omega plate reader (BMG LABTECH GmbH, Germany). A FEI Tecnai G^2 twin transmission electron microscope (Hillsboro, OR) was used to acquire transmission electron microscopy (TEM) micrographs. Particle size distributions were measured by Nanoparticle Tracking Analysis (NTA) on a NanoSight NS500 (Amesbury, UK).

2.3. Gold Nanostar Synthesis (AuNS). Three types of AuNS were synthesized as previously reported.[7] A 12 nm gold seed solution was prepared by adding 15 mL of 1% trisodium citrate to 100 mL of a boiling solution of 1 mM $HAuCl_4$. This solution was kept boiling for an additional 15 min, cooled to room temperature in an ice bath, filtered through a 0.22 μm nitrocellulose membrane, and stored at 4 °C until use. To produce the AuNS, 100 μL of the gold seed was added to a 10 mL solution of 0.25 mM $HAuCl_4$ containing 10 μL of 1 N HCl, immediately followed by the simultaneous addition of 50 μL 0.1 M AA and 100 μL of $AgNO_3$ (0.5, 1, or 3 mM; samples designated S5, S10, and S30 based upon the final concentration of $AgNO_3$) under moderate stirring. The concentration of the silver nitrate solution controls the branch length and branch number of the resulting AuNSs. After synthesis, 100 μL of 0.1 M CTAB was added to the AuNS solution and left stirring for 5 min. The particles were then centrifuged at 2000 rcf for 20 min at 4 °C, the supernatant was discarded, and the particles were redispersed in 10 mL of 1 mM CTAB solution.

2.4. Gold Nanosphere Synthesis (AuNP). CTAB stabilized AuNPs were obtained by the method of Jana et al.[14] Gold seed was prepared by the addition of 0.6 mL of freshly prepared, ice-cold $NaBH_4$ to a 20 mL aqueous solution containing 0.25 mM $HAuCl_4$ and 0.25 mM trisodium citrate. Growth solution (0.25 mM $HAuCl_4$ in 0.08 M aqueous CTAB) was prepared while the seed particles were aged for 2 h. Seeded growth was performed by mixing 7.5 mL of growth solution with 50 μL 0.1 M AA and then adding 2.5 mL of the gold seed solution while stirring; this is designated set A. After 10 min, 1 mL of set A was added to 9 mL of growth solution containing 50 μL of 0.1 M AA, producing set B. This process was repeated two more times to obtain sets C and D. The particles from set D are ∼30 nm in diameter and were used for subsequent silver coating. Set D was washed three times by centrifugation (3000 rcf for 30 min at 4 °C) and redispersion in 1 mM CTAB solution.

2.5. Silver Coating of Gold Nanoparticles (AuNS@Ag and AuNP@Ag). A 1 mL aliquot of the washed AuNS/AuNP solution was transferred into a 1.5 mL centrifuge tube. The sample was briefly vortexed after each subsequent chemical addition. A small volume (varied between 0 and 15 μL) of 0.1 M $AgNO_3$ and an equivalent volume of 0.1 M AA were added to the solution. The reduction of silver by AA was initiated by the addition of NH_4OH (2 μL), at which point the color of the solution began to darken. After about 5 min, the solution color had stabilized, indicating completion of the reaction. The various silver-coated AuNS samples were designated according to the volume of $AgNO_3$ added (e.g., S30@Ag5 for S30 AuNS coated using 5 μL of 0.1 M $AgNO_3$). The silver-coated AuNS was then labeled with dye by adding 1 μM final concentration of the desired dye (dissolved in MeOH) to the solution, allowing it to sit for 15 min, centrifuging at 2000 rcf for 10 min, discarding the supernatant, and redispersing in water.

2.6. Silica Coating (AuNS@Ag@SiO_2). Silica was coated onto the labeled AuNS@Ag using an established protocol.[15] To the 1 mL sample of dye-labeled particles prepared above, 5 μL of 1 mM mPEG-SH was added and allowed to react for 1 h. The solution was washed once by centrifugation (2500 rcf, 10 min) and then dispersed in 900 μL of EtOH with 200 μL of water. Silica coating was initiated by adding 18 μL of NH_4OH followed by 5 μL of 10% TEOS in EtOH to the solution. The reaction was allowed to proceed for 12 h, at which point the sample was washed twice by centrifugation at 3000 rcf for 5 min and redispersed in water.

2.7. Silver-Coated Nanostar 2D Modeling. The 2D simulations were performed using COMSOL Multiphysics 4.3b with the RF module. The gold AuNS model consisted of a 50 nm core, with six equally spaced branches of ∼25 nm in length. The silver coating process was modeled by overlaying increasingly larger spheres of silver onto the AuNS, until it became completely embedded in the silver shell. The dielectric functions of gold and silver were calculated using the Lorentz−Drude model from Johnson and Christy.[16] The nanoparticles were excited with an *x*-polarized plane wave propagating along the *y*-axis in the wavelength range from 400 to 800 nm.

2.8. SERS Nanoprobe Injections. A shaved rat pelt was provided by Dr. Bruce Klitzman. Prior to injection, 1 mL of AuNS@Ag@SiO_2 was centrifuged at 3000 rcf for 5 min and the supernatant discarded. The particles were then redispersed in 100 μL of PBS, giving a particle concentration of about 1 nM. A 1 mL disposable syringe with a 27G needle was used to draw up ∼50 μL of the PBS particle solution. The needle was inserted tangentially to the skin (intradermal) with the bevel facing upward, and ∼25 μL of the solution was injected. The rat pelt was then placed under the focus of the Raman probe to collect SERS spectra.

dx.doi.org/10.1021/jp4091393 | J. Phys. Chem. C 2014, 118, 3708−3715

3. RESULTS AND DISCUSSION

3.1. Synthesis and SERS Characterization. The AuNSs used in this study were prepared according to our previous report.[17] To better characterize the silver coating process, three types of NSs were prepared: S5, which have low branch numbers and length, an average particle size around 50 nm, and an extinction maximum at 650 nm; S10, which have low branch numbers with an increased branch length, an average particle size around 60 nm, and an extinction maximum at 750 nm; and S30, which have high branching, an average particle size around 70 nm, and an extinction maximum at 850 nm. The particles are designated by the final concentration of $AgNO_3$ (used to control the branching) in the reaction mixture (e.g., S30 is prepared with 30 μM final concentration of $AgNO_3$). After synthesis, CTAB was added as a surfactant to stabilize the particles, which were then purified by centrifugation to remove any unreacted reagents.

Silver coating of the NSs was performed in a similar manner to previous reports on the coating of gold nanorods with silver and modified from our previous method for gold seeded growth of monodisperse silver nanospheres.[18,19] In this study, the CTAB-stabilized AuNSs are used as seeds for the growth of a silver shell. Ascorbic acid serves as the reducing agent, with silver nitrate used as the precursor to elemental silver. After adding AA and $AgNO_3$ to the AuNS seed solution, NH_4OH is introduced to increase the pH, initiating the reduction of Ag^+ to Ag^0 by AA. An immediate color change is observed after the pH adjustment. The extinction maximum of the solution begins to blue-shift from the NIR region. After about 5 min, the color of the solution stabilizes, indicating completion of the silver coating reaction. A range of silver-coated samples were prepared, from 0 to 15 μL of 0.1 M $AgNO_3$ added per mL of NS solution. These samples are referred to by the NS type@Ag#, where the # is the volume of silver added in μL per mL of NS solution; thus, 1 mL of S10 coated using 5 μL 0.1 M $AgNO_3$ solution would be designated S10@Ag5.

To understand the silver coating process, we used S10 as a model where the coating process was monitored by UV/vis spectroscopy and TEM. Figure 1 shows the extinction spectra

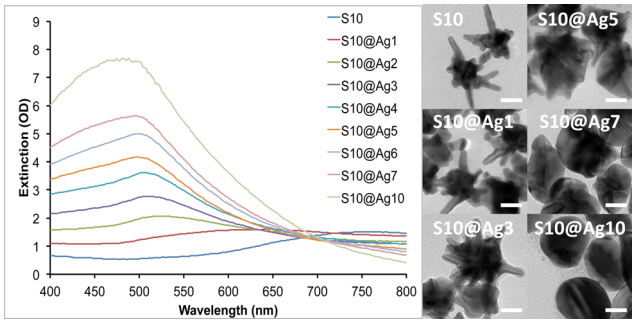

Figure 1. Extinction spectra of S10 with increasing silver coating (left). TEM images of the corresponding S10@Ag samples (right). Scale bars are 25 nm.

of S10 coated with various amounts of silver, along with TEM images of a few representative samples. The plasmon band of the S10 progressively blue-shifts from around 750 nm down toward 500 nm as the amount of silver coating is increased. We have previously shown that the NIR plasmon maximum position of AuNSs is mainly controlled by the aspect ratio of the branches protruding from the core.[7] Upon silver addition, it can be seen from the TEM images that the coating develops from NS core and expands outward. This process effectively decreases the aspect ratio of the branches that protrude from the silver shell, resulting in the observed blue-shift in their plasmon maximum and decreased plasmon intensity in the NIR range.

To further investigate the observed plasmon shift, theoretical modeling using the finite element method in COMSOL Multiphysics was performed. A 2D AuNS model was designed with a 50 nm core and six equally spaced branches of 25 nm in length. To simulate the silver coating process, increasingly larger spheres of silver were overlaid upon the AuNS core. The radius of the silver spheres used ranged from 30 to 50 nm, in steps of 5 nm. A plane wave polarized in the x-direction, traveling along the y-axis, was used to excite the particle in the wavelength range of 400−800 nm, evaluated in 10 nm steps. As can be seen in Figure 2, the theoretical model shows the same

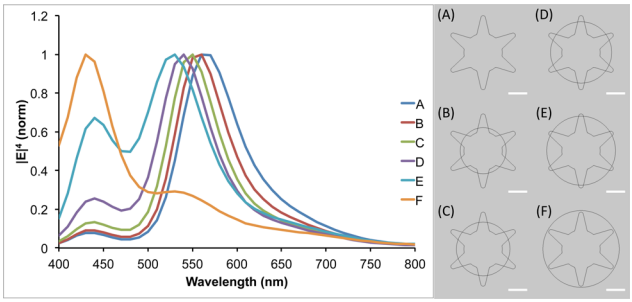

Figure 2. Simulated $|E|^4$ as a function of wavelength for the models shown on the right. An x-polarized plane wave traveling along the y-axis was used for excitation. The value of $|E|^4$ was calculated at the tip of the upper-right branch in the particle models. Scale bars are 25 nm.

trend as the experimental data, with the plasmon blue-shifting as the amount of silver is increased. The two plasmon peaks seen in the simulation can be attributed to the core for the shorter wavelength peak and the branches for the longer wavelength peak. This model also shows a decrease in the intensity of the branch plasmon peak relative to the core plasmon peak as the size of the silver shell is increased, which is in agreement with the experimental spectra.

For SERS intensity evaluation, we chose to compare the overall SERS brightness of the nanoparticle samples in lieu of calculating their enhancement factors, which tend to be inaccurate as a consequence of assumptions made in their determination.[1] Factors that would interfere with an enhancement factor calculation for these particles include the irregular shape of the nanoparticles making it difficult to calculate their surface area to determine the number of dye molecules that can bind per particle, the use of CTAB leading to more than a monolayer of dye coverage per particle, and self-absorption of the particles reducing the measured Raman signal.[11,12]

The SERS properties of these S10@Ag were then examined and compared with silver-coated gold nanospheres (AuNP@Ag). The AuNP were prepared by a seeded growth method in CTAB solution. UV/vis extinction spectra and TEM images of the AuNP can be found in Figure S1. All samples were labeled with 1 μM of DTDC and allowed to sit for 15 min before SERS measurements. Figure 3 shows the collected spectra from the various S10@Ag (Figure 3A) and AuNP@Ag (Figure 3B). The AuNP@Ag exhibit much lower SERS than S10@Ag, which is to be expected if the particles are in a nonaggregated state.[1,6] Note

dx.doi.org/10.1021/jp4091393 | J. Phys. Chem. C 2014, 118, 3708−3715

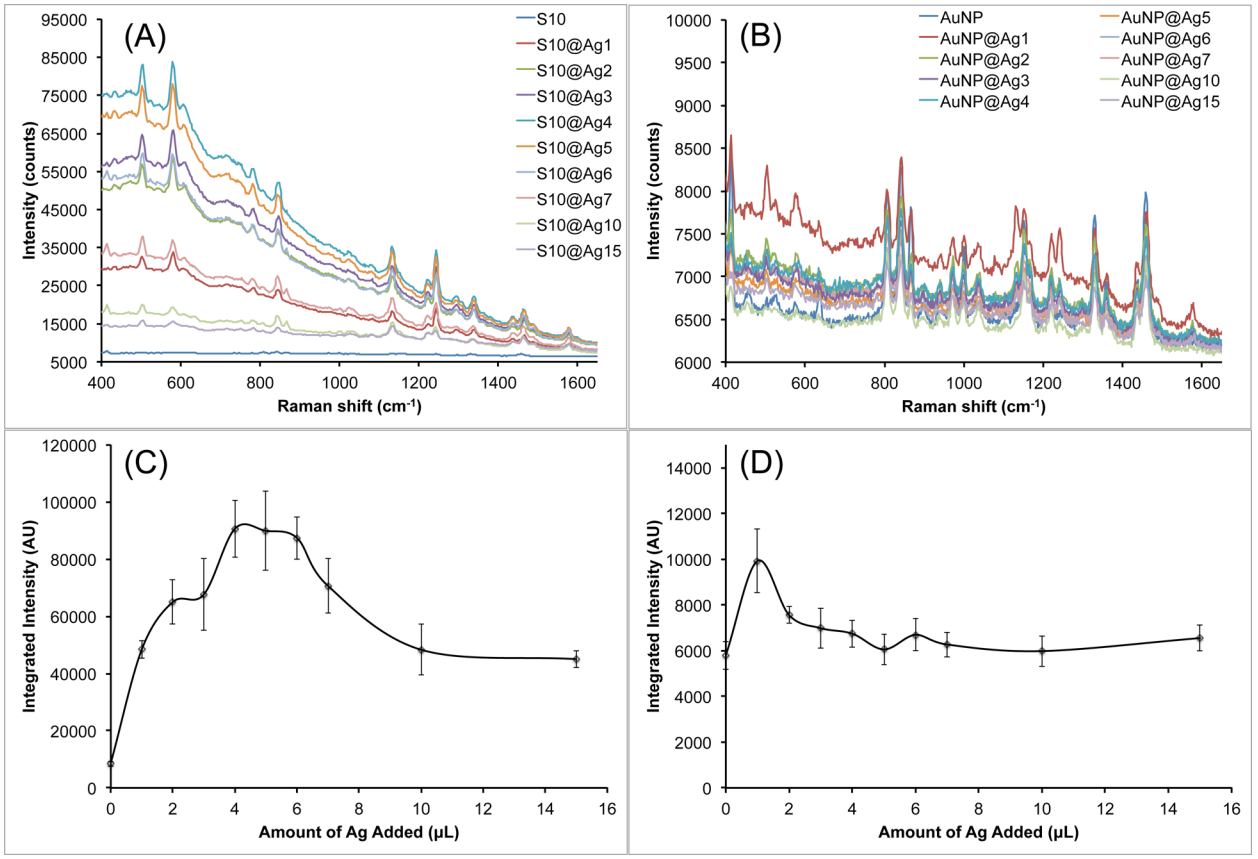

Figure 3. Raw SERS signal intensity of S10@Ag (A) and AuNP@Ag (B) samples with different amounts of silver coating. Spectra were acquired with a 1 s exposure time at 785 nm (150 mW power at the sample). Because of the low SERS intensity, spectra from AuNP@Ag contain visible background from the plastic vials used during the measurements. The integrated intensity of the DTDC peak around 1580 cm^{-1} is shown below the spectra for the S10@Ag (C) and AuNP@Ag (D) samples. Error bars are ±1 standard deviation (n = 7).

that the signal intensity from the S10@Ag can be an order of magnitude higher than that of the AuNP@Ag. To more accurately compare the SERS intensities, the spectra were background subtracted and then the intensity of the peak around 1580 cm^{-1} was integrated. The integrated intensities for the S10@Ag and AuNP@Ag samples are shown in Figures 3C and 3D, respectively. The maximum enhancement for the S10@Ag is found at S10@Ag4, with an 11 ± 2 times increase in signal intensity than S10 alone. The AuNP@Ag exhibit a maximum enhancement at AuNP@Ag1, with a 2.2 ± 0.3 times increase in signal.

To examine the contribution of attenuation due to extinction on the observed increase in SERS intensity, ethanol was used as an internal standard to normalize the measured spectra. Since the ethanol Raman peaks are not enhanced by the nanoparticles, any observed intensity variation can be attributed to changes in the extinction of the solution near the laser wavelength. Silver-coated S10 samples were prepared and labeled with pMBA. The pMBA dye was chosen for this study due to its thiol functionality, which will keep the dye molecules tightly bound to the nanoparticle surface in the presence of ethanol. Each sample was spiked to contain 10% ethanol before SERS measurements were performed. Spectra were acquired with a 1 s exposure time at 785 nm with 250 mW power at the sample. Figure 4 shows the integrated signal intensity recorded for the pMBA peak at ~1580 cm^{-1} (Figure 4A), the ethanol peak at ~880 cm^{-1} (Figure 4B), and the normalized pMBA peak intensity (Figure 4C). The maximum SERS brightness is observed around Ag5, which is similar to what was shown above in Figure 3. The Raman signal from the ethanol internal standard behaves as expected, which increases as the AuNS plasmon is progressively blue-shifted away from the laser wavelength. When the intensity of the pMBA peak is normalized by that of the ethanol, the measured SERS brightness actually decreases as more silver is added. This suggests that reduced attenuation, achieved by blue-shifting the nanostar plasmon away from the laser excitation wavelength, plays a significant role in the SERS signal enhancement that is observed in Figure 3. The silver coating itself may also be contributing to the enhanced un-normalized SERS brightness; however, single-particle SERS measurements would need to be performed to investigate this effect, which is beyond the scope of this study.

3.2. AuNS Comparison and SERRS Evaluation. To compare the SERRS variation among different types of AuNSs, S5 and S30 were also evaluated to validate the synthesis method and experimental observations as obtained with the S10. Figure 5 shows the progression of S5@Ag and S30@Ag of increasing amounts of silver. As previously observed, the silver deposition begins mainly on the core of the particles, spreading outward as the amount of silver is increased until the branches are completely covered, resulting in a quasi-spherical shape. The smaller S5 are shown to have their branches mostly covered at lower amounts of silver than the larger S30. Magnified views of uncoated S30 and S30@Ag7 are shown in Figure S2, clearly showing branches of the NSs protruding from the silver shell.

dx.doi.org/10.1021/jp4091393 | J. Phys. Chem. C 2014, 118, 3708−3715

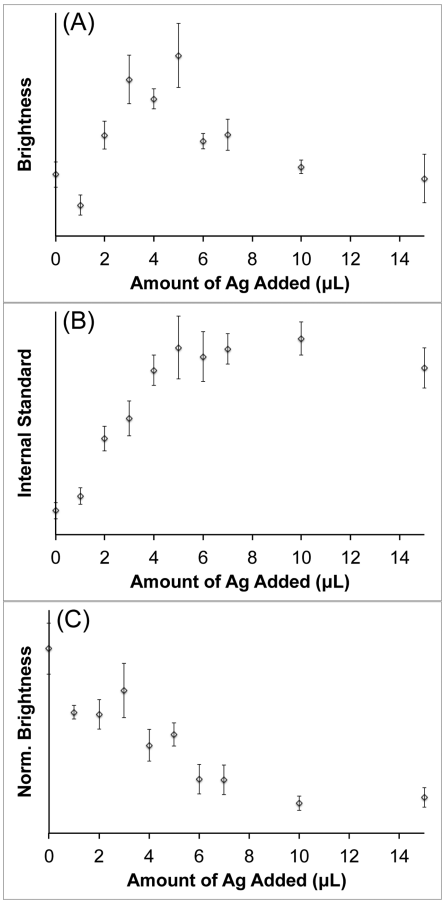

Figure 4. Recorded signal intensity of the pMBA peak at ~1580 cm^{-1} (A), the ethanol peak at ~880 cm^{-1} (B), and the ethanol normalized pMBA signal (C). Spectra were recorded at 785 nm, 250 mW, 1 s exposure. Error bars are ±1 standard deviation (n = 7).

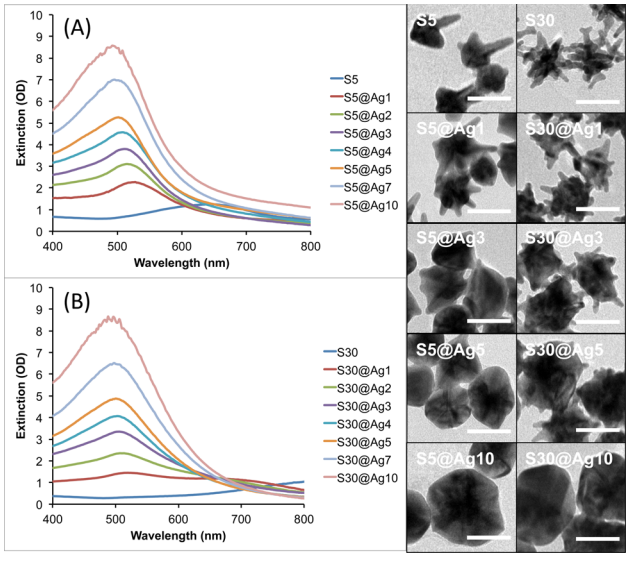

Figure 5. UV/vis extinction spectra of S5@Ag (A) and S30@Ag (B) of varying amounts of silver coating, as indicated in the legends, accompanied by representative TEM micrographs for both types of NS. Scale bars are 50 nm.

Figure 5 shows the extinction spectra for both S5@Ag and S30@Ag as the amount of silver is varied. The S5 plasmon is around 650 nm while the S30 plasmon is around 850 nm; in both cases, the extinction maximum blue-shifts to ~500 nm and increases in intensity with increasing amounts of silver. Note that there is no peak observed at ~420 nm, where the plasmon peak of silver nanospheres occurs, suggesting no nucleation of silver particles. The blue-shifting NS plasmon, along with the absence of a plasmon peak at ~420 nm, is indicative of silver shell formation on the AuNS.

To fabricate the SERS nanoprobes with the highest brightness, several factors were taken into consideration. Resonant SERS was employed because it generates multiple orders of magnitude higher SERRS signal than nonresonant SERS on nonaggregated AuNSs. In addition, we have shown that when using resonant dyes, a plasmon that is blue-shifted from the excitation provides the highest signal, as self-absorption effects are minimized when the plasmon is off-resonance from the excitation.[11] Previously, we used sodium dodecyl sulfate (SDS) as a surfactant on AuNS to aid in stabilization and dye adsorption. It is believed that the hydrophobic bilayer formed by the SDS helps to entrap dyes near the particle surface. We have found that CTAB can act in the same manner and exhibits about 2−3 times higher signal intensity than particles stabilized with SDS. The longer hydrophobic chain of CTAB (16 carbons) versus SDS (12 carbons) likely provides a larger volume for trapping dye molecules.

To investigate the effect of the various silver coatings on resonant Raman enhancement, AuNS@Ag samples were labeled with a NIR resonant dye, IR-780, for surface-enhanced resonant Raman scattering (SERRS) measurements. Figure 6 shows the SERRS brightness of S5@Ag and S30@Ag with various amounts of silver. The raw SERRS spectra of S5@Ag (Figure 6A) and the integrated, background-subtracted signal intensity at 730 cm^{-1} (Figure 6B) are shown. At its highest brightness, with S5@Ag3, the signal is enhanced 16 ± 2 times over the S5. For S30@Ag (Figure 6C,D), the highest intensity is observed at S30@Ag7, which is 9 ± 1 times higher than the signal of S30. It is worth noting that the maximal SERRS brightness was found on AuNSs with subtotal silver coating. Correlated with the TEM images from Figure 5, it is apparent that the maximum Raman signal enhancement occurs right before the gold tips become completely embedded in the silver shell. More silver does not always lead to higher SERRS response. A near-total silver coverage retains the hotspots from the AuNS tips while lowering self-absorption from the NS solution to yield the strongest SERRS. In contrast, spherical silver coating with a mismatched plasmon maximum but no sharp tips had a SERRS brightness that was only slightly greater than the initial NS sample.

To ensure these nanoprobes were not aggregated, which would cause anomalously high Raman signals, the size distributions of S30@Ag were evaluated by NTA, both before and after dye labeling (Figure S3). No significant increase in particle size was observed after dye labeling, adding confidence that the particles remained in a nonaggregated state. The observed drop-off in Raman signal intensity after a certain amount of silver coating further supports the claim that particles remain nonaggregated after dye labeling. Once the ideal amount of silver coating is surpassed, the mostly spherical-shaped particles can be prone to aggregation, which would cause a marked increase in Raman signal.

The amount of sliver coating required for optimal SERRS appears to depend on the AuNS used. Although the exact amount of silver is not available in this study, the progression in

dx.doi.org/10.1021/jp4091393 | J. Phys. Chem. C 2014, 118, 3708−3715

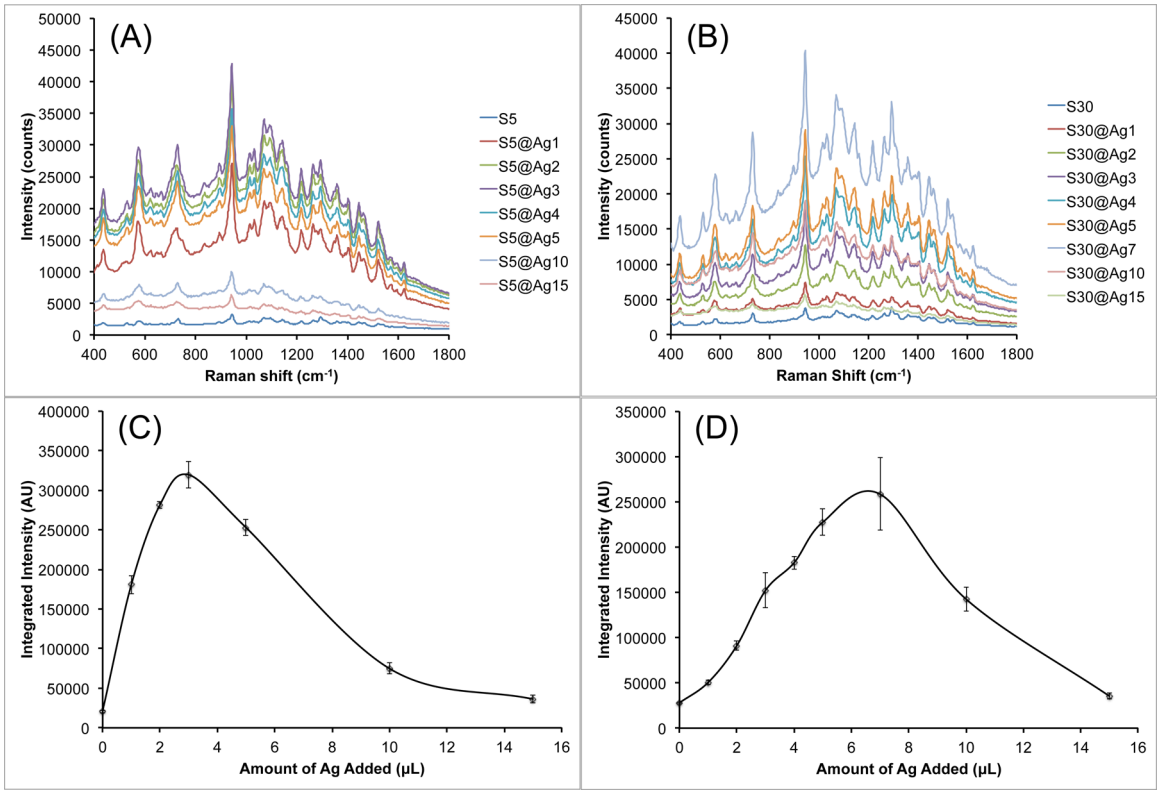

Figure 6. SERRS measurement of S5@Ag (A, C) and S30@Ag (B, D) with various amounts of silver coating, labeled with IR-780. Raw SERRS spectra for S5@Ag (A) and S30@Ag (B) are shown. Spline chart of the background-subtracted integrated signal intensity at 730 cm^{-1} for S5@Ag (C) and S30@Ag (D) samples. Error bars are ±1 standard deviation (n = 3). All spectra were recorded with a 100 ms exposure time using a 785 nm laser (150 mW power at the sample).

the extinction spectra and TEM images clearly characterize the silver amount semiquantitatively. Among the three types of NSs, they vary in core size, branch length, and number. Based on the TEM findings, the particle geometry (e.g., core size and branch length/number) may dictate the required silver amount to obtain subtotal coverage on the AuNS for optimal SERRS. With S5 having a smaller core and few broad branches, the amount of silver required for subtotal coverage is less than that from S30, having a larger core and more sharp branches. The actual amount of silver coating required for optimal SERS/SERRS, however, needs to be determined experimentally based on particle size and shape.

3.3. SERS Nanoprobe for Bioapplications. In order to make SERS/SERRS nanoprobes suitable for bioapplications, it is necessary to encapsulate the particles in an inert material, e.g., silica. Coating the Raman nanoprobes with silica protects the dye on the particle surface for greater structural stability and prevents unwanted adsorption of other molecules that may generate their own Raman signal. We prepared SERS nanoprobes using three different carbocyanine dyes (DTDC, DTTC, and HITC) to demonstrate the potential for multiplex detection. Thiol-PEG was used to stabilize the particles when transferred into ethanol for silica coating by a modified Stöber method.[20] The PEG layer also acts to facilitate silica condensation onto the surface of the particles, presumably through hydrogen bonding.[15] This method was found to be equally effective at encapsulating both AuNS@Ag and bare AuNS. The measured particle size distribution (Figure S4) showed no obvious signs of aggregation after silica coating. Figure 7 compares the Raman signal intensity from silica-coated, DTTC-labeled S30 and S30@Ag7. It is shown that after silica coating,

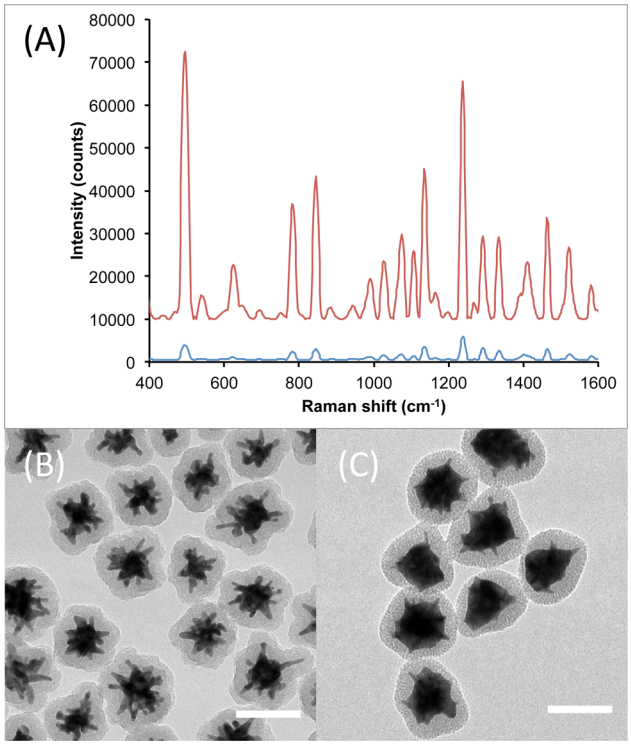

Figure 7. Comparison of Raman signal intensity from S30-DTTC@SiO_2 (A, blue) and S30@Ag7-DTTC@SiO_2 (A, red), collected with a 100 ms exposure time. The spectra have been background subtracted and offset for clarity. TEM micrographs of the Ag0 and Ag7 SERS nanoprobes are shown in (B) and (C), respectively. Scale bars are 100 nm.

dx.doi.org/10.1021/jp4091393 | J. Phys. Chem. C 2014, 118, 3708−3715

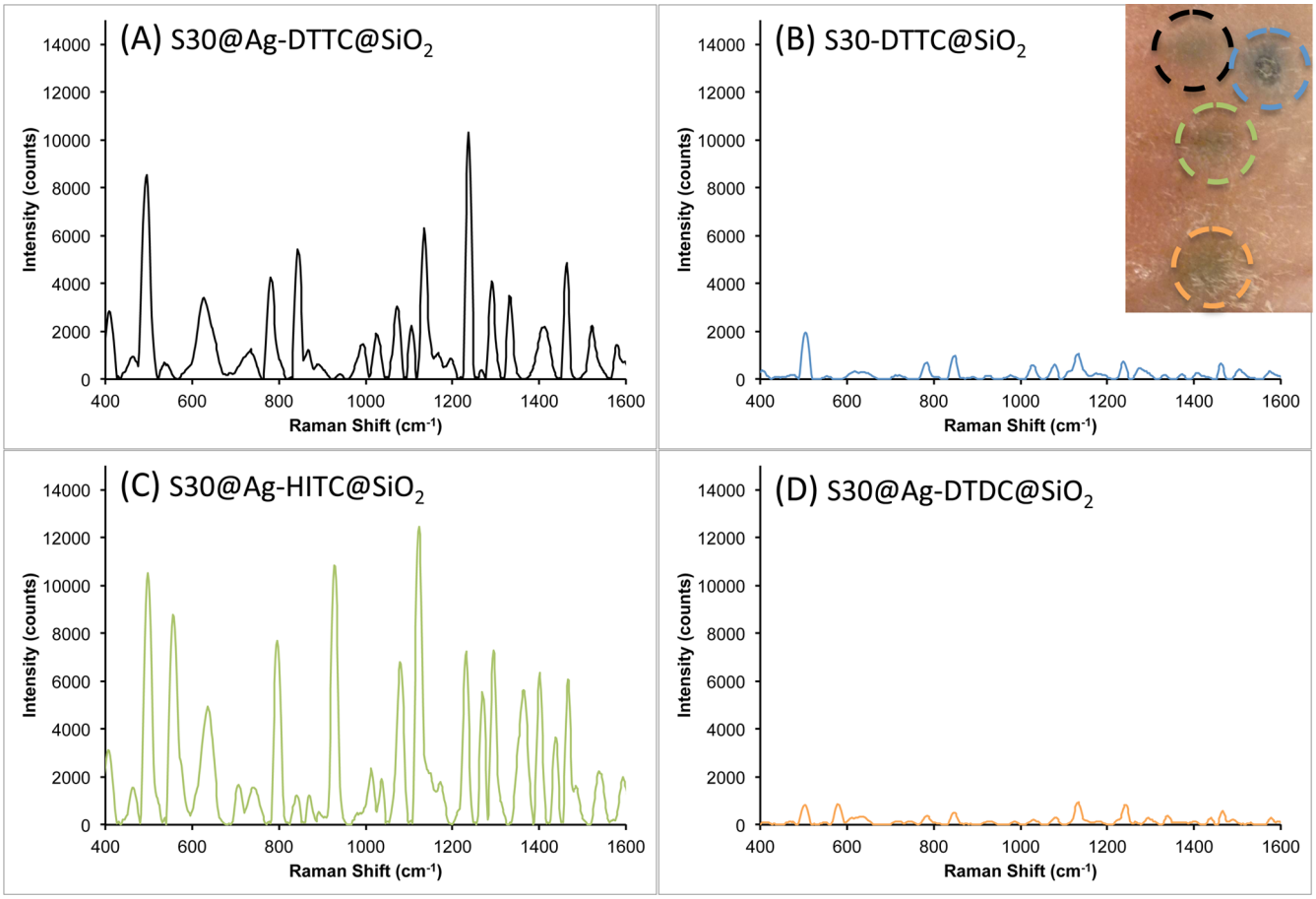

Figure 8. Raman spectra (background subtracted) recorded from different SERS nanoprobes after intradermal injection into a rat pelt: (A) S30@Ag7-DTTC@SiO_2, black; (B) S30-DTTC@SiO_2, blue; (C) S30@Ag7-HITC@SiO_2, green; (D) S30@Ag7-DTDC@SiO_2, orange. The inset at top right shows the injection sites, each outlined in the color that matches the corresponding spectrum above.

the order of magnitude in signal difference between the S30 and S30@Ag7 is maintained. The TEM micrographs show that both particle types were completely coated and in a non-aggregated state.

To show the potential of our new AuNS@Ag in biological applications, the prepared SERS nanoprobes were injected into a rat pelt for *ex vivo* detection. To prepare the particles for injection, the solutions were concentrated 10 times and dispersed in sterile PBS. The particle solutions were drawn up into 1 mL syringes with a 27G needle. About 25 μL of each SERS nanoprobe was injected into the skin at different locations. The injection volume produced a small welt, with the particle solutions clearly visible through the skin (figure inset). Note that the injection of the nonsilver coated nanoprobe looks darker than the others because of the original solution color; the AuNS solution is a dark gray color while the AuNS@Ag solution is reddish-orange. The injection area was then swabbed with an alcohol pad before optical interrogation with the Raman probe.

As seen in Figure 8, three AuNS@Ag@SiO_2 (DTTC, HITC, and DTDC) and one AuNS@SiO_2 (DTTC) were measured through the dermis. The S30@Ag7-DTTC@SiO_2 (Figure 8A) showed a higher signal-to-noise ratio than the S30-DTTC@SiO_2 (Figure 8B), demonstrating stronger SERRS from S30@Ag@SiO_2 than from S30@SiO_2. The difference in signal intensity from resonant (DTTC and HITC) and nonresonant (DTDC) dyes is shown in Figure 8, with the resonant dyes providing an order of magnitude higher signal than the nonresonant dye. Also, nonresonant S30@Ag-DTDC@SiO_2 has comparable intensity as the resonant S30-DTTC@SiO_2. SERRS on AuNS@Ag@SiO_2 clearly has stronger signal intensity than its nonresonant SERS and non-silver-coated counterparts.

Another benefit of the AuNS@Ag SERRS nanoprobes is that the extinction maximum no longer occurs in the region of the laser excitation. When the plasmon peak matches the laser wavelength, a small area of burnt tissue can be seen in the center of the AuNS@SiO_2 injection site (blue circle, Figure 8 inset) after the measurement had been performed (150 mW power, 1 mm spot size, ~20 s exposure). The laser power at the sample had to be decreased below 40 mW in order to prevent any visible damage when measuring the AuNS-based probes. In contrast, no adverse effects on the tissue were seen for the AuNS@Ag@SiO_2 after laser interrogation, even under 250 mW for 20 s. Importantly, the photothermal effect did not affect the SERS signal of the particles over this period of time, even when the laser power was increased to 250 mW (Figure S5). It should be noted that there are many variables that could affect the observed photothermal response, including depth of the particle injection, concentration of the particle solution, volume of solution injected, and the type and pigmentation of skin. Therefore, although matching the laser excitation to the surface plasmon resonance of nanoparticles will generate the highest electromagnetic field enhancement for SERS, we show here

dx.doi.org/10.1021/jp4091393 | *J. Phys. Chem. C* 2014, 118, 3708−3715

that this is not always desirable, as doing so can lead to unintended tissue damage, along with extinction-based attenuation of SERS signal.

4. CONCLUSIONS

In this report we describe in detail the synthesis, characterization, and application of a novel hybrid bimetallic platform, AuNS@Ag, for SERS/SERRS detection. The amount of silver coating was optimized to blue-shift the plasmon while retaining the hotspots on sharp tips, hence giving the greatest SERS/SERRS brightness. The morphology of the particles was assessed by TEM, while the optical properties were characterized with UV/vis spectroscopy and Raman spectroscopy. In the optimized configuration, AuNS@Ag provided over an order of magnitude of signal enhancement compared to uncoated AuNS. The enhancement is most likely due to the off-resonance plasmon that reduces background self-extinction. Silica-coated, dye-labeled AuNS@Ag and AuNS were prepared for entrapping the dyes and preserving the nonaggregated state of the particles. To demonstrate the potential for these particles in biolabeling applications, *ex vivo* detection was performed following intradermal injection of the SERS/SERRS nanoprobes into a rat pelt. Raman signal was detected from all three AuNS@Ag nanoprobes, and the measurements did not cause any noticeable photothermal damage, which could occur when the particles' surface plasmon resonance coincide with the incident light. These new, ultrabright SERS particles will be further developed for sensing and imaging applications.

■ ASSOCIATED CONTENT

Supporting Information

Figures S1−S5. This material is available free of charge via the Internet at http://pubs.acs.org.

■ AUTHOR INFORMATION

Corresponding Author

*Ph (919) 660-8520, Fax (919) 613-9145, e-mail tuan.vodinh@duke.edu (T.V.-D.).

Notes

While this manuscript was under revision, a report by Samal et al. was published, describing a similar method that was capable of coating AuNSs with silver.[21] The authors declare no competing financial interest.

■ ACKNOWLEDGMENTS

This work was sponsored by the Duke University Exploratory Research Funds and the Defense Advanced Research Projects Agency (HR0011-13-2-0003). A.M.F. was supported by a training grant from the National Institutes of Health (T32 EB001040). The content of this article does not necessarily reflect the position or the policy of the Government, and no official endorsement should be inferred. The authors acknowledge Dr. Christopher G. Khoury for design of the COMSOL AuNS model.

■ REFERENCES

(1) Moskovits, M. Persistent Misconceptions Regarding SERS. *Phys. Chem. Chem. Phys.* **2013**, *15* (15), 5301−5311.

(2) Yuan, H.; Register, J.; Wang, H.-N.; Fales, A.; Liu, Y.; Vo-Dinh, T. Plasmonic Nanoprobes for Intracellular Sensing and Imaging. *Anal. Bioanal. Chem.* **2013**, *405* (19), 6165−6180.

(3) Barbosa, S.; Agrawal, A.; Rodríguez-Lorenzo, L.; Pastoriza-Santos, I.; Alvarez-Puebla, R. N. A.; Kornowski, A.; Weller, H.; Liz-Marzán, L. M. Tuning Size and Sensing Properties in Colloidal Gold Nanostars. *Langmuir* **2010**, *26* (18), 14943−14950.

(4) Nalbant Esenturk, E.; Hight Walker, A. R. Surface-Enhanced Raman Scattering Spectroscopy via Gold Nanostars. *J. Raman Spectrosc.* **2009**, *40* (1), 86−91.

(5) Khoury, C. G.; Vo-Dinh, T. Gold Nanostars for Surface-Enhanced Raman Scattering: Synthesis, Characterization and Optimization. *J. Phys. Chem. C* **2008**, *112* (48), 18849−18859.

(6) Yuan, H.; Fales, A. M.; Khoury, C. G.; Liu, J.; Vo-Dinh, T. Spectral Characterization and Intracellular Detection of Surface-Enhanced Raman Scattering (SERS)-Encoded Plasmonic Gold Nanostars. *J. Raman Spectrosc.* **2013**, *44* (2), 234−239.

(7) Yuan, H.; Khoury, C. G.; Hwang, H.; Wilson, C. M.; Grant, G. A.; Vo-Dinh, T. Gold Nanostars: Surfactant-Free Synthesis, 3D Modelling, and Two-Photon Photoluminescence Imaging. *Nanotechnology* **2012**, *23* (7), 075102.

(8) Fales, A. M.; Yuan, H.; Vo-Dinh, T. Silica-Coated Gold Nanostars for Combined Surface-Enhanced Raman Scattering (SERS) Detection and Singlet-Oxygen Generation: A Potential Nanoplatform for Theranostics. *Langmuir* **2011**, *27* (19), 12186−12190.

(9) Fales, A. M.; Yuan, H.; Vo-Dinh, T. Cell-Penetrating Peptide Enhanced Intracellular Raman Imaging and Photodynamic Therapy. *Mol. Pharmacol.* **2013**, *10* (6), 2291−2298.

(10) Liu, Y.; Yuan, H.; Fales, A. M.; Vo-Dinh, T. pH-Sensing Nanostar Probe Using Surface-Enhanced Raman Scattering (SERS): Theoretical and Experimental Studies. *J. Raman Spectrosc.* **2013**, *44* (7), 980−986.

(11) Yuan, H.; Liu, Y.; Fales, A. M.; Li, Y. L.; Liu, J.; Vo-Dinh, T. Quantitative Surface-Enhanced Resonant Raman Scattering Multiplexing of Biocompatible Gold Nanostars for in Vitro and ex Vivo Detection. *Anal. Chem.* **2012**, *85* (1), 208−212.

(12) Sivapalan, S. T.; DeVetter, B. M.; Yang, T. K.; van Dijk, T.; Schulmerich, M. V.; Carney, P. S.; Bhargava, R.; Murphy, C. J. Off-Resonance Surface-Enhanced Raman Spectroscopy from Gold Nanorod Suspensions as a Function of Aspect Ratio: Not What We Thought. *ACS Nano* **2013**, *7* (3), 2099−2105.

(13) Wang, Y.; Yan, B.; Chen, L. SERS Tags: Novel Optical Nanoprobes for Bioanalysis. *Chem. Rev.* **2012**, *113* (3), 1391−1428.

(14) Jana, N. R.; Gearheart, L.; Murphy, C. J. Seeding Growth for Size Control of 5−40 nm Diameter Gold Nanoparticles. *Langmuir* **2001**, *17* (22), 6782−6786.

(15) Fernández-López, C.; Mateo-Mateo, C.; Álvarez-Puebla, R. N. A.; Pérez-Juste, J.; Pastoriza-Santos, I.; Liz-Marzán, L. M. Highly Controlled Silica Coating of PEG-Capped Metal Nanoparticles and Preparation of SERS-Encoded Particles. *Langmuir* **2009**, *25* (24), 13894−13899.

(16) Johnson, P. B.; Christy, R. W. Optical Constants of the Noble Metals. *Phys. Rev. B* **1972**, *6* (12), 4370−4379.

(17) Yuan, H.; Khoury, C. G.; Wilson, C. M.; Grant, G. A.; Bennett, A. J.; Vo-Dinh, T. In Vivo Particle Tracking and Photothermal Ablation Using Plasmon-Resonant Gold Nanostars. *Nanomedicine: NBM* **2012**, *8* (8), 1355−1363.

(18) Chen, S.; Liu, D.; Wang, Z.; Sun, X.; Cui, D.; Chen, X. Picomolar Detection of Mercuric ions by Means of Gold-Silver Core-Shell Nanorods. *Nanoscale* **2013**, *5* (15), 6731−6735.

(19) Garcia-Leis, A.; Garcia-Ramos, J. V.; Sanchez-Cortes, S. Silver Nanostars with High SERS Performance. *J. Phys. Chem. C* **2013**, *117* (15), 7791−7795.

(20) Stöber, W.; Fink, A.; Bohn, E. Controlled Growth of Monodisperse Silica Spheres in the Micron Size Range. *J. Colloid Interface Sci.* **1968**, *26* (1), 62−69.

(21) Samal, A. K.; Polavarapu, L.; Rodal-Cedeira, S.; Liz-Marzán, L. M.; Perez-Juste, J.; Pastoriza-Santos, I. Size Tunable Au@Ag Core-Shell Nanoparticles: Synthesis and SERS Properties. *Langmuir* **2013**, *29*, 15076−15082.